Controlling Fano lineshapes in plasmon-mediated light coupling into a substrate

P. Spinelli,* C. van Lare, E. Verhagen, and A. Polman

Center for Nanophotonics, FOM Institute AMOLF
Science Park 104, 1098 XG, Amsterdam, The Netherlands
**spinelli@amolf.nl*

Abstract: Metal nanoparticles are efficient resonant plasmonic scatterers for light, and, if placed on top of a high-index substrate, can efficiently couple light into the substrate. This coupling, however, strongly depends on particle shape and surrounding environment. We study the effect of particle shape and substrate refractive index on the plasmonic resonances of silver nanoparticles and we systematically relate this to the efficiency of light scattering into a substrate. The light coupling spectra are dominated by Fano resonances for the corresponding dipolar and quadrupolar scattering modes. Varying the particle shape from spherical to cylindrical leads to large shifts in the Fano resonance for the dipolar mode, reducing the light incoupling integrated over the AM1.5 spectral range. Using a dielectric spacer layer, good light coupling is achieved for cylinders in the near-infrared. An asymmetric environment around the particles turns quadrupolar resonances into efficient radiators as well.

OCIS codes: (240.6680) Surface plasmons; (040.5350) Photovoltaic.

References and links

1. G. Mie, "Beitrge zur Optik trber Medien, speziell kolloidaler Metallsungen," Ann. Phys. **330**(3), 377–445 (1908).
2. C. F. Bohren and D. R. Huffman, *Absorption and Scattering of Light by Small Particles* (Wiley, 2008).
3. H. A. Atwater and A. Polman, "Plasmonics for improved photovoltaic devices," Nat. Mater. **9**, 205–213 (2010).
4. H. R. Stuart and D. G. Hall, "Absorption enhancement in silicon-on-insulator waveguides using metal island films," Appl. Phys. Lett. **69**(16), 2327–2329 (1996).
5. H. R. Stuart and D. G. Hall, "Island size effects in nanoparticle-enhanced photodetectors," Appl. Phys. Lett. **73**(26), 3815–3817 (1998).
6. D. M. Schaadt, B. Feng, and E. T. Yu, "Enhanced semiconductor optical absorption via surface plasmon excitation in metal nanoparticles," Appl. Phys. Lett. **86**(6), 063106 (2005).
7. D. Derkacs, S. H. Lim, P. Matheu, W. Mar, and E. T. Yu, "Improved performance of amorphous silicon solar cells via scattering from surface plasmon polaritons in nearby metallic nanoparticles," Appl. Phys. Lett. **89**(9), 093103 (2006).
8. P. Matheu, S. H. Lim, D. Derkacs, C. McPheeters, and E. T. Yu, "Metal and dielectric nanoparticle scattering for improved optical absorption in photovoltaic devices," Appl. Phys. Lett. **93**(11), 113108 (2008).
9. K. R. Catchpole and A. Polman, "Design principle for particle plasmon enhanced solar cells," Appl. Phys. Lett. **93**(19), 191113 (2008)
10. K. R. Catchpole and A. Polman, "Plasmonic solar cells," Opt. Express **16**(26), 21793–21800 (2008).
11. S. H. Lim, W. Mar, P. Matheu, D. Derkacs, and E. T. Yu, "Photocurrent spectroscopy of optical absorption enhancement in silicon photodiodes via scattering from surface plasmon polaritons in gold nanoparticles," J. Appl. Phys. **101**(10), 106309 (2007).
12. B. Luk'yanchuk, N. I. Zheludev, S. A. Maier, N. J. Halas, P. Nordlander, H. Giessen, and C. T. Chong, "The Fano resonance in plasmonic nanostructures and metamaterials," Nat. Mater. **9**, 707–715 (2010).

#142694 - $15.00 USD Received 14 Feb 2011; revised 18 Mar 2011; accepted 21 Mar 2011; published 12 Apr 2011

13. C. Hägglund, M. Zch, G. Petersson, and B. Kasemo, "Electromagnetic coupling of light into a silicon solar cell by nanodisk plasmons," Appl. Phys. Lett. **92**(5), 053110 (2008).
14. Lumerical FDTD Solutions (www.lumerical.com).
15. http://www.lumerical.com/fdtd_online_helpprevious_help/user_guide_tfsf_sources.php.
16. E. D. Palik, *Handbook of Optical Constants of Solids* (Academic, 1985).
17. U. Kreibig and M. Vollmer, *Optical Properties of Metal Clusters* (Springer, 1995).
18. J. Mertz, "Radiative absorption, fluorescence, and scattering of a classical dipole near a lossless interface: a unified description," J. Opt. Soc. Am. B **17**(11), 1906–1913 (2000).
19. F. J. Beck, A. Polman, and K. R. Catchpole, "Tunable light trapping for solar cells using localized surface plasmons," J. Appl. Phys. **105**(11), 114310 (2009).
20. G. Xu, M. Tazawa, P. Jin, S. Nakao, and K. Yoshimura, "Wavelength tuning of surface plasmon resonance using dielectric layers," Appl. Phys. Lett. **82**(22), 3811–3813 (2003).

1. Introduction

Metal nanoparticles have attracted much interest for their optical properties, which are very different from those of bulk material. The strong surface plasmon resonance (SPR) of these particles results in strong optical scattering and a strongly enhanced optical near-field around the particle [1, 2]. Recently, the scattering properties of metal nanoparticles are being investigated as a possible way to achieve light trapping in thin-film solar cells [3]. It has been shown experimentally [4–8] and numerically [9, 10] that arrays of metal nanoparticles placed on the surface of a substrate can enhance the transmission of light into the substrate.

From a fundamental point of view, it has been shown that Fano resonances play an important role in light incoupling into a substrate, reducing light transmission for frequencies below resonance due to destructive interference between scattered and incident light [11, 12]. Thus, good control of the scattering properties is needed in order to maximize the incoupling of light into a substrate for different wavelengths. Recent studies have investigated light scattering from metal nanoparticles of different material, size, shape and placed in different dielectric environment. We have shown earlier that cylindrical and hemispherical particles have a better near-field coupling to the substrate than spherical particles, due to the reduced spacing between the effective dipole moment and the substrate [9]. In another paper, Hägglund *et al.* propose that small spherical particles, rather than cylinders, are closer to the ideal shape for efficient light scattering into a substrate, due to the better coupling of the dipolar-like resonance of a sphere with respect to the quadrupolar-like resonance of a cylinder [13].

In this paper we clarify to what extent the near-field distribution of the particle modifies its scattering properties and thus the light incoupling into the substrate. By using Finite Difference Time Domain (FDTD) simulations, we analyze how the scattering efficiency spectrum is modified when the particle shape is gradually changed from a sphere to a cylinder and when the refractive index of the substrate is gradually increased. We systematically compare the scattering cross section spectrum with the total transmission spectrum, showing that an increase in transmission occurs at wavelengths above each scattering resonance, while a reduction occurs below resonance. In the last part of the paper, we use these results for photovoltaic applications. Cylindrical particles are found to be less efficient for light incoupling in the visible and near infra-red than spheres, due to a strongly red-shifted dipolar resonance. The introduction of a transparent dielectric spacer layer can re-establish efficient light transmission in the near infrared even for cylinders by blue-shifting the dipole resonance, an aspect that is relevant for experimental fabrication procedures.

2. Shape and environment effect on plasmonic resonance

We start our analysis by calculating the scattering cross section of silver nanoparticles on crystalline silicon, by means of FDTD calculations [14]. The simulation setup is shown in the inset

#142694 - $15.00 USD Received 14 Feb 2011; revised 18 Mar 2011; accepted 21 Mar 2011; published 12 Apr 2011

of Fig. 1. A single silver nanoparticle is placed on the top of a semi-infinite silicon substrate. Perfectly Matched Layers (PMLs) are used at the boundaries of the simulation volume to prevent non-physical scattering at the boundaries. The simulation box size is 1×1×0.8 μm^3. A mesh size of 1 nm is used in the entire region containing the particle and at the substrate-air interface, and a smaller (0.2 nm) mesh grid is used around the sharp features at the particle-substrate contact point. We use a "Total-Field Scattered-Field" (TFSF) source [15] to simulate a broadband (wavelength 300-1100 nm) plane wave pulse incident on the particle from the top.). Usually, the scattering cross section is calculated in FDTD by placing frequency-domain monitors in the "scattered-field" region of a TFSF source. In this case, the presence of an absorbing substrate implies that part of the field does not reach the "scattered-field" region, due to absorption in the substrate. For this reason, we use a time-domain field monitor positioned 1 nm below the Si surface and we calculate the spectrum of the power scattered in the Si with a Fourier transform of the field measured by this time-domain monitor, after subtracting the incident field. The total power transmitted into the substrate, which will be analyzed in the next section, is directly measured by a frequency-domain monitor placed 1 nm below the Si surface. Optical constants for Ag were taken from Palik [16] and fitted using a Drude-Lorentz model; data for Si were taken from Palik as well.

The Ag particle is defined by a cylindrical body and two spheroids, one on top and one at the bottom, whose horizontal radius matches the radius of the cylinder (see inset in Fig. 1(a)). The shape of the particle is changed by varying the round edge parameter h, i.e. the vertical radius of the spheroids. The volume and the in-plane diameter of the particle are kept constant when varying the shape (thus the particle height changes) to ensure the same scattering volume.

Figure 1(a) shows the scattering cross section spectrum, normalized to the geometrical cross section, for three different particle shapes: a sphere (green), a cylinder with a 10 nm round edge (red) and a cylinder with sharp edge (h = 0 nm, blue). We observe that all spectra present two resonances. The quadrupole resonance around 450 nm wavelength does not shift when varying the particle shape. On the contrary, the dipole resonance is strongly red-shifted when the shape is changed from a sphere (resonance at 500 nm) to a 10 nm round edge particle (800 nm) to a cylindrical particle (resonance out of range of the graph, above 1100 nm). Note that the small oscillations in the scattering cross section spectra are the result of hot-spots in the contact region of the particle with the substrate, due to the finite size of the mesh grid in the simulation setup.

In order to understand the origin of the different resonances that appear in the spectra for the three different shapes, we study the scattering cross section starting from the very simple, but instructive case of a single silver nanoparticle in homogenous medium. For spherical particles, Maxwell's equations can be solved exactly, and the scattering cross section can be calculated using Mie theory [1]. For particles of different shape, FDTD calculations were performed.

Figure 2 shows the normalized scattering cross section (indicated by the gray scale) as a function of wavelength and (a) particle size, (b) surrounding refractive indices, and (c) particle shape. The latter is once again defined by the round edge parameter shown in the inset of Fig. 1(a). The trends seen in Fig. 2(a) and 2(b) are all well known [2, 17]: as the particle size (Fig. 2(a)) or the refractive index of the surrounding medium (Fig. 2(b)) increases higher-order multipolar modes appear (dipole, quadrupole, octupole, etc.), and all resonances red shift and broaden, due to increased retardation across the particle. Varying paricle shape (Fig. 2(c)) we notice a small red-shift of the dipolar and quadrupolar resonance, when the particle shape is changed from a sphere (75 nm round edge, top of the graph) to a cylinder (0 nm round edge, bottom of the graph), which we attribute to slightly enhanced retardation across the particle.

The next step is to analyze how the scattering cross section of particles of different shapes changes when a substrate is introduced. Mie theory can no longer be used, due to the breaking of the symmetry in the surrounding environment. Thus, we use FDTD simulations to calculate

#142694 - $15.00 USD Received 14 Feb 2011; revised 18 Mar 2011; accepted 21 Mar 2011; published 12 Apr 2011

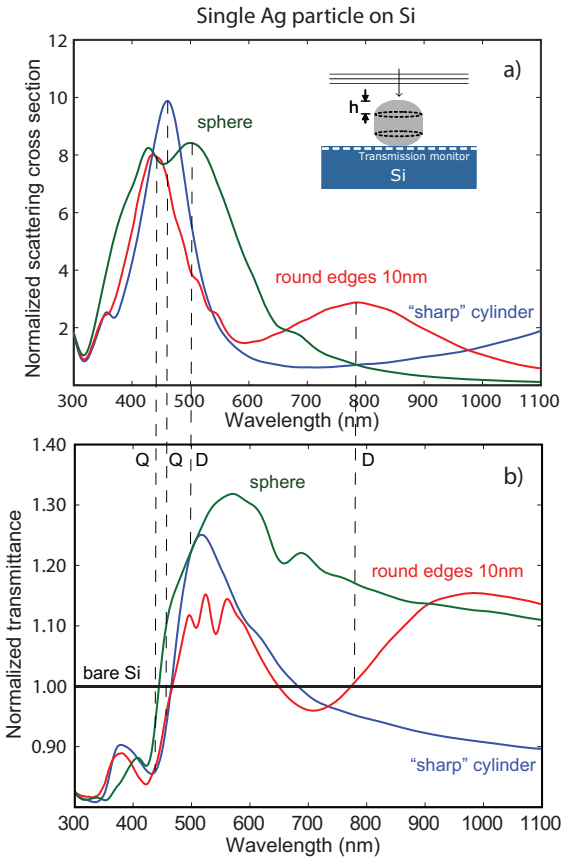

Fig. 1. Normalized scattering cross section spectra (a), and normalized transmittance (b) for particles of three different shapes on top of a crystalline Si substrate. The dipole resonance is strongly red-shifted when particle shape is changed from a sphere (green), to a 10 nm round edge cylinder (red), to a sharp edge cylinder (blue). The normalized transmittance spectrum shows a reduction below each resonance, due to the Fano effect. The inset in (a) shows the simulation geometry. Data are calculated for a box size of $1\times1\times0.8\ \mu m^3$. The peak resonance wavelengths are indicated by the dashed vertical lines.

#142694 - $15.00 USD Received 14 Feb 2011; revised 18 Mar 2011; accepted 21 Mar 2011; published 12 Apr 2011

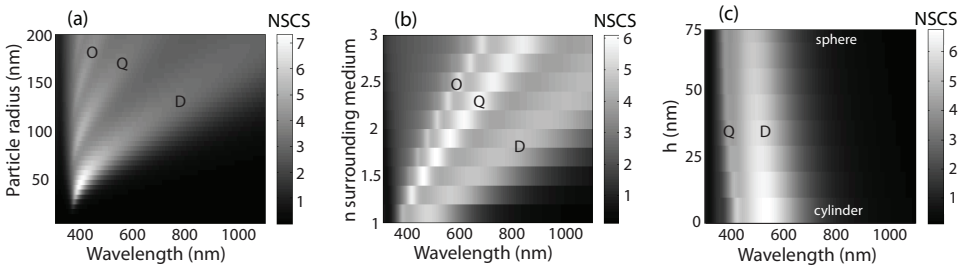

Fig. 2. Normalized scattering cross section (NSCS) spectra (gray scale) for a Ag sphere in air as a function of particle size (a), for a 150 nm diameter Ag sphere as a function of different surrounding refractive index (b), and for a nanoparticle in air as a function of the round edge parameter *h* (c). Panels (a) and (b) are calculated using Mie theory; panel (c) is the result of FDTD calculations. A redshift of the resonances is observed as the particle size or the surrounding refractive index increase and when the shape is changed from a sphere to a cylinder. Dipolar (D), quadrupolar (Q) and octupolar (O) resonances are indicated.

the scattering efficiency.

Figure 3 shows the normalized scattering cross section (gray scale) for a sphere (a), a 10 nm round edge cylinder (b) and a sharp edge cylinder (c), as a function of wavelength and substrate index. The three particle shapes clearly show different trends. In the case of a spherical

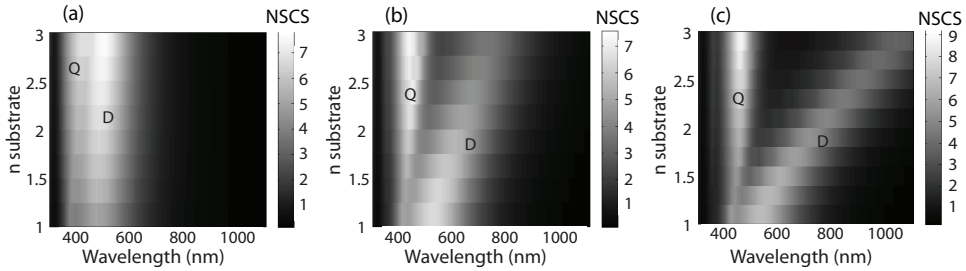

Fig. 3. Normalized scattering cross section spectra (NSCS, gray scale) for a sphere (a), a 10 nm round edge cylinder (b) and for a sharp cylinder (c), all with an in-plane diameter of 150 nm, as a function of the substrate refractive index. A redshift of the dipolar resonance is observed as the substrate index increases. This effect is very large for cylindrical particles. The quadrupolar resonance is only slightly affected by the presence of the substrate.

particle (Fig. 3(a)), both the dipolar and the quadrupolar resonance are nearly unaffected by the presence of the substrate. On the other hand, for a 10 nm round edge cylinder (Fig. 3(b)) the graph shows a strong redshift for the dipolar resonance, whereas the quadrupole resonance is nearly unchanged. Finally, for a sharp cylinder (Fig. 3(c)), the redshift of the dipolar resonance is even larger; the quadrupolar peak is again nearly unaffected.

In order to understand the origin of the large red-shift of the dipolar resonance of the cylindrical particle on a substrate, we investigate the field distribution inside the cylinder at the resonance wavelengths. Figure 4 shows the scattered field distribution at dipole (a) and quadrupole (b) resonance in air, and at dipole (c) and quadrupole (d) resonance on a n=3 substrate. The scattered field is obtained subtracting the incident field from the total field. As can be seen, the presence of a high-index substrate changes the field distribution of particle at resonance. For the dipole resonance, the symmetric field distribution of a particle in air (a) is turned in a dipolar-like field distribution at the interface with the substrate (c). On the contrary, for the

#142694 - $15.00 USD Received 14 Feb 2011; revised 18 Mar 2011; accepted 21 Mar 2011; published 12 Apr 2011

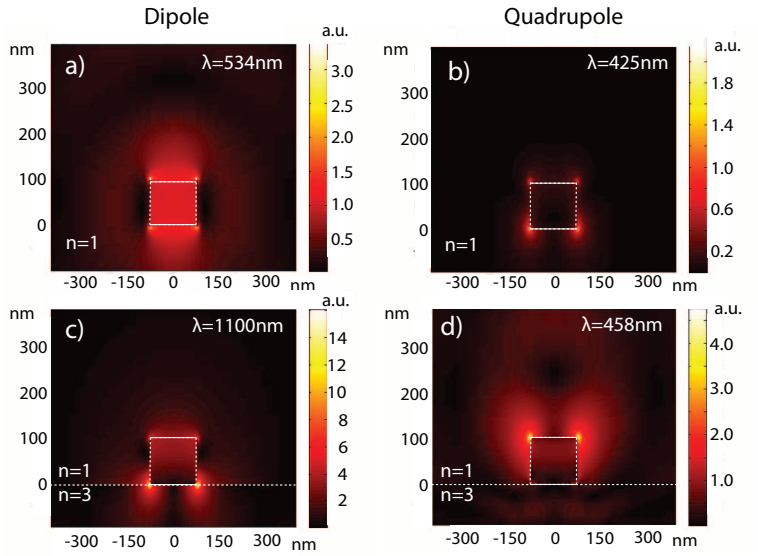

Fig. 4. Scattered electric field intensity distribution for the dipolar (a) and quadrupolar (b) resonance in air and for the dipolar (c) and quadrupolar (d) resonance for a 150 nm diameter cylinder on a n=3 substrate. The presence of the substrate strongly modifies the field distribution of the particle at resonance. The field distribution due to the dipolar resonance is located at the interface with the substrate, whereas the quadrupolar resonance field is located at the particle-air interface.

quadrupole resonance, the symmetric field plot in air (a) turns into a dipolar-like distribution at the particle-air interface (d). This result is in agreement with the observation of Hägglund *et al.* [13].

For this reason, the dipolar resonance residing at the particle-substrate interface, is more sensitive to the changes in the local environment when the substrate index is increased, thus resulting in the pronounced red shift shown in Fig. 3(c). The quadrupolar resonance, on the other hand, is less sensitive to the change of substrate index, as the corresponding field is located at the particle-air side. Thus, its resonance wavelength is only slightly changed when the substrate index is increased.

3. Effect on light incoupling into a substrate

The results obtained above on the scattering cross section spectra for different shapes and substrate index are closely related to the efficiency of light incoupling into a substrate by metal nanoparticles. We study the light incoupling into a silicon substrate by means of FDTD calculations. The simulation setup is shown in the inset of Fig. 1(a): a frequency-domain monitor positioned just below the surface measures the total power that is coupled into the Si (transmission).

Figure 1(b) shows the transmission spectrum of a single Ag nanoparticle on top of Si, normalized to the transmission spectrum of a bare Si substrate. Note that the absolute values of the normalized transmittance depend on the simulation box size, which is 1×1×0.8 μm^3 in this case. The small features present in these spectra are again attributed to the finite mesh size of the simulation setup. The dashed lines between Figs. 1(a) and 1(b) correspond to the dipole and quadrupole resonance peak wavelengths.

The graph shows that in spectral ranges above resonance the transmission is enhanced by the

#142694 - $15.00 USD Received 14 Feb 2011; revised 18 Mar 2011; accepted 21 Mar 2011; published 12 Apr 2011

presence of the nanoparticle. The mechanism behind this effect is the preferential scattering of light at the particle resonance into the high-index substrate, due to the higher density of states in the substrate [18]. This enhancement is seen for both the dipolar and quadrupolar mode for the sphere and rounded cylinder in Fig. 1(b); for the sharp cylinder the dipole resonance is outside the range of the graph. In contrast, a clear reduction of the incoupled power occurs below each resonance. This reduction occurs due to a Fano effect, i.e. a destructive interference between scattered and incident light occurring at wavelengths below resonance [11].

The shift of the plasmon resonance to the red occurring when the shape is changed from a sphere to a cylinder, leads to a broadening of the Fano reduction for wavelengths below resonance. For a sharp cylinder, with the dipolar resonance above 1100 nm, the reduction in transmission becomes very broadband (see Fig. 1(b)).

4. Example: plasmon-enhanced light coupling into c-Si solar cells

Clearly, the use of metal nanoparticles to increase transmission into the substrate requires a careful choice of particle shape, depending on the wavelength of interest, in order to tune the effect of these Fano resonances on the incoupling. From now on, we focus on the metal nanoparticles of these arrays for photovoltaic applications.

Figure 5 shows the wavelength integrated transmission calculated for different values of the round edge parameter, ranging from 0 nm (sharp cylinder) to 75 nm (sphere), normalized to transmission for bare Si, by integrating over the AM1.5 solar spectrum from 300 to 1100 nm. The enhancement factor is thus an index of how good the incoupling of sunlight into the Si solar cell is. The graph clearly shows an increase in the enhancement factor as the shape is

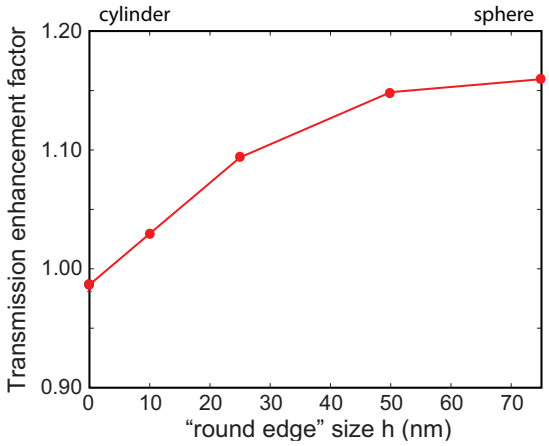

Fig. 5. Transmission enhancement factor, calculated by integrating transmission spectra such as in Fig. 1(b) over the AM1.5 solar spectrum, normalized to a bare Si substrate, as a function of the round edge parameter. Spherical particles (75 nm round edge) show better incoupling of light than cylindrical particles (0 nm round edge). The simulation box size is $1\times1\times0.8\ \mu m^3$.

varied from a cylinder to a sphere. The lower value for a sharp edge cylinder is explained by the broadband Fano reduction below the dipolar resonance in the infrared region (Fig. 1(b)). As the particle is made rounder and rounder, the dipolar resonance is shifted towards the blue, and the Fano reduction becomes less significant. Thus, the transmission enhancement factor increases.

The data presented in Fig. 5 show that for bare particles placed on a Si substrate a round

#142694 - $15.00 USD Received 14 Feb 2011; revised 18 Mar 2011; accepted 21 Mar 2011; published 12 Apr 2011

shape is better than a cylindrical one. We now solve the controversy with literature regarding the optimal shape. Catchpole *et al.* showed that cylindrical shapes show better near-field coupling into the substrate than a sphere. Our work shows that this comes at the expense of a large red-shift of the Fano resonance, which when integrated over the solar spectrum is detrimental, leading to the spherical shape as the preferred one, in agreement with Hägglund's prediction.

It has already been shown that the introduction of a dielectric spacer layer between particles and substrate yields a blue-shift of the dipole resonance [19, 20]. However, the effect of this shift on the light coupling to a substrate taking into account the Fano interference has not been studied so far. Figure 6 shows the effect on the scattering cross sections and on the transmission spectra of introducing a Si_3N_4 (n=2.00) dielectric spacer layer between a cylindrical Ag nanoparticle and the Si substrate. The upper panel (Fig. 6(a)) shows the scattering cross section

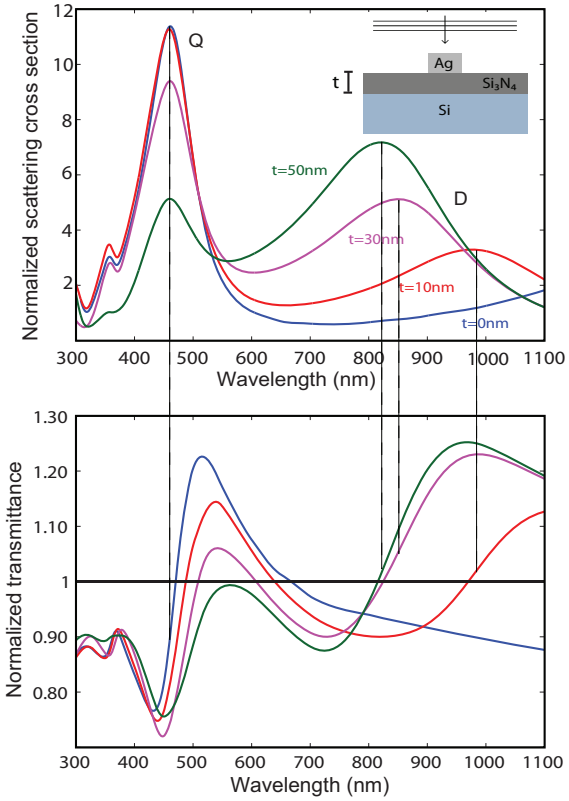

Fig. 6. Normalized scattering cross section (a) and normalized transmittance (b) spectra for a cylindrical Ag particle on top of Si (blue) and on top of 10 nm (red), 30 nm (purple) and 50 nm (green) thick Si_3N_4 layer. Data in (b) are normalized to the transmission for a Si substrate with the corresponding Si_3N_4 layer thickness. The dipolar resonance is shifted to the blue as the Si_3N_4 layer thickness is increased. The normalized transmittance spectrum shows a reduction below each resonance, due to the Fano effect.

of a cylindrical (0 nm round edge) Ag nanoparticle directly on Si (blue), and on top of a 10 nm (red), 30 nm (purple) and 50 nm (green) thick Si_3N_4 spacer layer. The lower panel (Fig. 6(b)) shows the normalized transmission spectrum for the same geometries. Note that in this case the reference is different for each curve, as the transmission has been normalized to the case of a Si substrate with a Si_3N_4 layer on top, with the corresponding thickness. This normaliza-

#142694 - $15.00 USD Received 14 Feb 2011; revised 18 Mar 2011; accepted 21 Mar 2011; published 12 Apr 2011

tion allows to isolate the effect due to the particle scattering only, corrected for the intrinsic anti-reflection effect due to the Si_3N_4 layer.

We observe a strong blue-shift of the dipolar resonance as the Si_3N_4 thickness is increased from 0 to 50 nm. This phenomenon is explained by the reduction of the effective index in the near-field region of the particle, which results in a shift of the resonance to lower wavelengths, as shown before (see Fig. 3(c)). As a consequence, an increase of the total transmission is observed in the near infra-red due to the narrowing of the range where the Fano related reduction is present.

This work also shows that creating a strong field asymmetry around the particle due to the presence of a high-index substrate can turn a quadrupole mode into an efficiently radiating mode. Interestingly, Fig. 6 also shows a strong reduction in the strength of the quadrupole resonance as the Si_3N_4 thickness is increased. This is due to the fact that for Ag particles that are strongly coupled to the Si substrate the quadrupole field distribution becomes more dipolar in nature (see Fig. 4) resulting in more effective radiation into the substrate. Thus, a thicker Si_3N_4 spacer layer causes enhanced transmission (compared to the bare Si_3N_4 case) in the infrared but reduced transmission in the visible.

5. Conclusion

We have systematically studied the effect of Ag particle shape and substrate on the plasmon mediated light coupling to a high-index substrate.The dipole resonance is strongly redshifted when the shape is changed from a sphere to a cylinder due to the increased near-field coupling of the dipolar field with the substrate. The Ag particles scatter preferentially into the substrate. We determine the transmission spectra for different shapes and compare these to the scattering spectra. Strong Fano-type lineshapes are observed in the transmission spectra, originating from the interference of the direct and scattered light fields. Destructive interference leads to reduced transmission below resonance and is then very sensitive to particle shape. The strong red-shift observed for cylindrical particles reduces the incoupling for a spectral band corresponding to the AM1.5 solar spectrum due to the Fano effect. The introduction of a dielectric spacer layer results in good light incoupling for the near-infrared also for cylindrical particles, by shifting the dipolar resonance to the blue. In a strongly asymmetric dielectric environment the quadrupole mode is an efficient radiator as well. The insights given in this paper clarify the role of near-field coupling and Fano resonances in the scattering of light and transmission of light into a substrate. These results open new perspectives for designing and fabricating metal nanoparticle arrays for light trapping in thin-film solar cells.

Acknowledgments

The authors are grateful to Femius Koenderink for the Mie theory MATLAB code. This work is part of the research program of the Foundation for Fundamental Research on Matter (FOM) which is financially supported by the Netherlands Organization for Fundamental Research (NWO). It is also part of the Global Climate and Energy Project (GCEP).

#142694 - $15.00 USD Received 14 Feb 2011; revised 18 Mar 2011; accepted 21 Mar 2011; published 12 Apr 2011